

## Investigation of the Association Between Imaging and Pathological Characteristics of HCC

Mansour Mohamed Kabbash<sup>1</sup>, Hussein Ali Mostafa<sup>1</sup>, Stephen Wigmore<sup>2</sup>,  
Sherif Elprince Sayed<sup>1</sup>, Abdelrahman Mohamed Kamel Amin\*<sup>1</sup>

<sup>1</sup>Department of General and Onco-surgery, Faculty of Medicine, Aswan University

<sup>2</sup>Department of Hepatobiliary Surgery, Faculty of Medicine, Edinburgh University

\*Corresponding author: Abdelrahman Mohamed Kamel Amin, Email: playsurgery@yahoo.com,

Mobile: (+20)01553596111

### ABSTRACT

**Background:** Hepatocellular carcinoma (HCC) is the most typical primary viscus malignancy and also the second leading reason behind cancer-related death worldwide.

**Objectives:** To study the association between the tomography and pathological options of HCC for getting an honest designation on the lesions of HCC for getting the best treatment and prognosis of these lesions.

**Patients and Methods:** Study of the imaging criteria of HCC which includes the arterial enhancement and venous washout in both CT and MRI within a background of cirrhosis, and it's a possible association with the vascular density and microvascular invasion seen in the biopsy. We enrolled consecutive cirrhotic patients with HCC liver resection in 2 years (from January 2018 till December 2019).

**Results:** Our results on the number of lesions cleared that, the number of lesions ranged from 1 in number that observed in 68 (66.02 %) and 2 that observed in 11 (10.68 %), followed by 3, 4, and 5 lesions that observed in 1 (0.97 %) of the examined patients. The higher incidences of the lesions observed in middle hepatic vein 55 (53.40 %) right lobe of the liver 16 (15.54 %), seg 2/3 10 (9.71 %), right liver 5 (4.86 %), left liver 5 (4.86 %) and in left lateral liver 4 (3.88 %).

**Conclusion:** The association between the Imaging and pathological features of HCC including microvascular invasion and density which is very important for getting an honest designation on the lesions of HCC and for getting the best treatment and prognosis of these lesions.

**Keywords:** HCC, CT, MRI, T2WI, HBP, DWI .

### INTRODUCTION

HCC usually originates from the cirrhotic liver <sup>(1)</sup>, with 2–8% of liver disease patients developing HCC annually. For accomplishment best treatment of HCC, we tend to should rely on the great designation of HCC for investigations of the feature of the HCC <sup>(2)</sup>.

The typical imaging options of HCC principally originate from the histopathologic characteristics of nodular progressed HCCs instead of those of early HCCs. Among the numerous pathophysiologic alterations that will occur throughout hepatocarcinogenesis, neovascularization is that the most significant part that helps to supply the characteristic imaging options of progressed HCCs <sup>(3)</sup>.

Recent tips, together with those of the European Association for the Study of the Liver and European Organization for analysis and Treatment of Cancer (EASL-EORTC), the yank Association for the Study of disease (AASLD), and also the Korean liver disease Study cluster and also the National Cancer Center (KLCSG-NCC), yield the noninvasive designation of HCC mistreatment contrast-enhanced X-radiation (CT), resonance imaging (MRI), or ultrasound (US) on the idea of its typical imaging options <sup>(4)</sup>.

The hallmark imaging options of HCC are blood vessel part hyperenhancement (APHE) and

portal/delayed washout, that represent the characteristic tube-shaped structure profile of HCC on dynamic CT or tomography <sup>(2)</sup>.

Indeed, these HCCs with atypical imaging options stay an enormous diagnostic challenge for radiologists nowadays. Moreover, in at-risk patients, there will be several HCC mimickers like intrahepatic cholangiocarcinoma (ICC), combined HCC-cholangiocarcinoma (cHCC-CC), arteriportal (AP) shunt, and hemangioma. Therefore, precise differentiation of HCCs from these mimickers on surgical imaging studies would be of nice clinical importance, guiding the suitable treatment strategy <sup>(5)</sup>.

HCCs may also show many different characteristic imaging options that will be useful in their differentiation from different benign liver lesions. First, neoplasm capsules are discovered in some seventieth of progressed HCCs with expandable growth <sup>(3)</sup>.

The capsule look is outlined as a peripheral rim sweetening discovered within the portal blood vessel or delayed phases of contrast-enhanced CT or tomography <sup>(6)</sup>. This capsular look ought to be differentiated from rim sweetening that's solely seen within the blood vessel part, which is common in cholangiocarcinoma (CC) or metastases from carcinoma <sup>(7)</sup>.



This article is an open access article distributed under the terms and conditions of the Creative Commons Attribution (CC BY-SA) license (<http://creativecommons.org/licenses/by/4.0/>)

The nodule-in-nodule design is another characteristic microscopic anatomy and radiologic feature of HCC. It's outlined because the presence of a smaller inner nodule with completely different imaging options from the larger outer nodule, suggesting the presence of a progressed HCC portion inside an abnormality nodule (DN) or Associate in Nursing early HCC <sup>(6)</sup>. Similarly, the mosaic design is additionally a vital characteristic imaging feature of enormous HCCs. This imaging feature refers to the presence of every which way distributed internal nodules or compartments typically separated by fibrous septations, showing completely different attenuation, signal intensity (SI), and sweetening pattern <sup>(7)</sup>.

Vascular invasion is additionally common in giant and/or best HCCs, and occlusion within the hepatic portal vein is reportable to occur in 44–62.8% of enormous HCCs <sup>(8)</sup>. A neoplasm coagulum will be known by its closeness with the first neoplasm Associate in Nursing shows a bent toward an expandable feature, enlargement of obstructed vessels, and increased neovascularity, leading to distinction sweetening <sup>(5)</sup>. Therefore, on dynamic CT and tomography, progressed HCCs usually show APHE followed by washout look on the portal or delayed phases <sup>(9)</sup>, in keeping with the Liver Imaging coverage and information system (LI-RADS), APHE is outlined as relative hyperenhancement as compared with the encompassing liver parenchyma, and washout is outlined as a non-peripheral, visually assessed temporal reduction within the degree of sweetening relative to composite liver tissue, leading to hypo enhancement within the portal blood vessel or delayed phases <sup>(2)</sup>.

When clinicians or radiologists encounter difficult cases within the cirrhotic liver, a careful interpretation ought to be performed mistreatment multiparametric imaging, together with T2WI, HBP, and DWI, additionally to the relative sweetening pattern seen on dynamic CT or tomography. additionally, the appliance of adjunct options following the LI-RADS diagnostic algorithmic program would be useful in creating an accurate designation in HCCs with atypical options whereas decreasing false-positive diagnoses <sup>(10, 11)</sup>.

**So, this study aimed** to study the association between the tomography and pathological options of HCC for getting an honest designation on the lesions of HCC for getting the best treatment and prognosis of these lesions.

## PATIENTS AND METHODS

Study of the imaging criteria of HCC which includes the arterial enhancement and venous washout in both CT and MRI within a background of cirrhosis, and it's a possible association with the vascular density and microvascular invasion seen in the biopsy. Data collection and statistics were held at the University of Edinburgh, UK.

Inclusion criteria involve patients with cirrhosis presenting by hepatic lesion with typical (arterial

enhancement and venous washout) and atypical (no enhancement or washout) features on imaging whatever the cause of cirrhosis. All patients had undergone Liver resection either open or laparoscopic from January 2018 till December 2019 at Royal Infirmary of Edinburgh, Department of Surgery, UK. Specimens have been analyzed at the Pathology Department including histopathology review and microvascular analysis.

The present study was approved in advance by the Ethical Committee of the University of Edinburgh, UK. All patients were treated according to the ethical guidelines of the 1975 Declaration; informed consent was obtained from each patient at the time of surgery.

We enrolled consecutive cirrhotic patients with HCC liver resection in 2 years (from January 2018 till December 2019). The inclusion criteria were: availability of clinical and MRI data performed, together with nodule tissue for histopathological and immunohistochemical (IHC) analyses.

## MRI techniques and image analysis:

In this study, MRI was performed using hepatospecific contrast media such as gadolinium ethoxybenzyl diethylenetriamine pentaacetic acid (EOB Primovist; Bayer Schering Pharma, Berlin, Germany). The images obtained by MRI were blindly reviewed by two board-certified radiologists with more than 10 years of experience in liver imaging and more than 10 years of specific experience in the use of hepatospecific contrast media in liver MRI. They were blinded to each other and any information regarding histopathological features.

The radiologist recorded the number of lesions, the longest diameter, and the liver location of each nodule. For each nodule, the signal intensity (1 = hyperintense; 2 = isointense; 3 = hypointense) was collected in T1 (in-phase and out-phase) and T2-weighted images and in arterial, portal-venous and hepatobiliary phase images. The diffusion-weighted image (DWI) signal intensity was collected as follows: 0 indicated that the lesion was not observed or was isointense (absence of restriction) and 1 that the lesion had some degree of hyperintensity from minimal perceptible hyperintensity to maximal hyperintensity similar to that of the spleen (presence of restriction).

## Histopathology and immunohistochemistry:

Tissue samples from the nodules were taken from the surgical LT specimen for routine histopathological analysis. From formalin-fixed and paraffin-embedded tissue blocks, 2- $\mu$ m-thick sections were cut for Hematoxylin-Eosin and Reticulin stains, as well as for IHC. At histological analysis, regenerative nodules (RN) were diagnosed as hepatocellular nodules with no cytological atypia, low cell density, and regular architecture; low-grade dysplastic nodules (LGDN) as nodules with slightly increased cell density. High-grade dysplastic nodules (HGDN) showed mild architectural and/or cytological atypia, an increased cell density, a progressive loss of portal tracts, and occasional unpaired arteries. Finally, early HCC (eHCC) showed stromal

invasion, increased nuclear/cytoplasmic ratio, trabecular architecture and/or acinar structures, several unpaired arteries, and eventually fatty changes. Definite HCC, tumor grade according to Edmondson, tumor architecture, and growth were evaluated, together with the occurrence of microvascular invasion (MVI).

### Determination of Microvascular density:

#### a-Stereological point counting:

All grid points overlapping with vessels (V) were counted, regardless of whether the microvessels crossed the left or bottom outer grid lines (Fig 1). A grid point, which was designated by two perpendicular cross-lines, was regarded as overlapping a microvessel when it fell on an endothelial cell or a vessel lumen (red arrows versus shaded red arrow in Fig 1). When, exceptionally, only a single endothelial cell of a larger vessel was stained, all other endothelial cells that lined this vessel

were nonetheless counted upon an intersection. To establish a reference area, all grid points intersecting with tissue (Vref) were counted. Small necrotic zones within tumor structures or glandular lumens were considered as cancer tissue. Only if more than 75% of the grid area (more than 60 out of the 81 grid points) covered tissue, the ROI was analyzed.

The unbiased estimation of the microvessel areal fraction was calculated for each sample according to  $A_A = (\sum V_i) / (\sum_i V_{i \text{ ref}})$ ; with  $i$  value from 1 to 15 ROIs, expressed as a percentage of microvessels per area, with  $V_i$  the number of grid points overlapping with vessels in ROI  $i$  and  $V_{i, \text{ref}}$  the number of grid points hitting tissue in ROI  $i$  <sup>(12)</sup>.

#### Error!

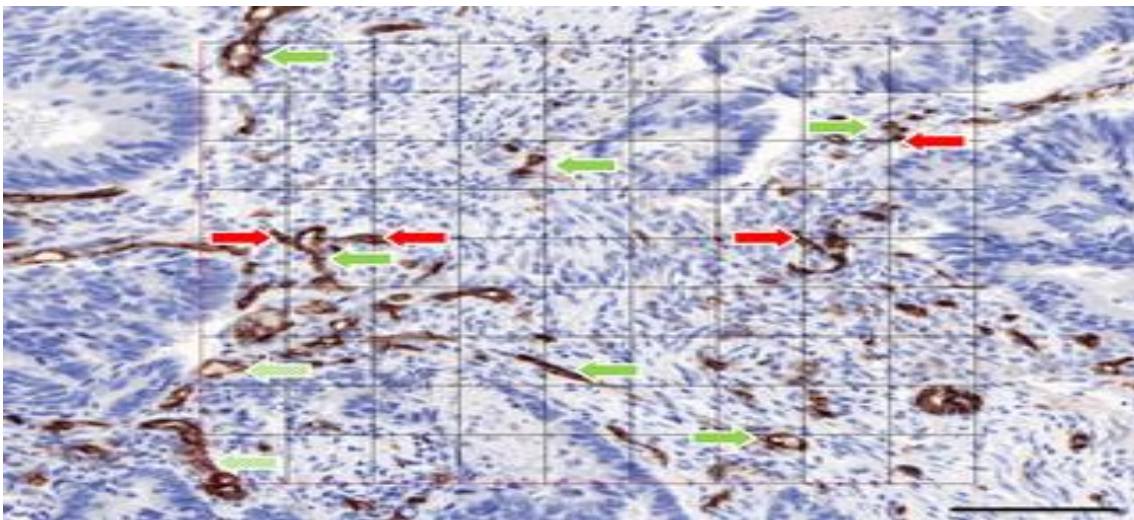


**Figure (1):** Example of a region of interest. CD31-stained vessel profiles in the grid were counted as N (green arrow). Vessel profiles that cross the virtually extended left or the lower line of the grid were not counted (shaded green arrow). The grid points that hit a CD31-stained vascular profile were counted as V (red arrow). Scale bar represents 100  $\mu\text{m}$ .

#### b-Microvessel counting:

Besides the stereological point counting, the microvessel density (QA) is captured by our method. The outer borders of the superimposed grid (Fig 1) <sup>(12)</sup>, delineated the counting chamber. Vascular structures crossing the virtually extended left or bottom lines of the grid were not counted. Regardless of staining, the others were counted (shaded green arrows in Fig 1) <sup>(13)</sup>. The initial counting rules only took into account stained structures with a clear lumen or without a lumen but larger than one tumor cell. Accordingly, very small cross-sectioned capillaries without a clear lumen were not counted. CD31 staining of suspected myofibroblast-like cells or cells not belonging to a blood vessel was also excluded for counting. Because of high inter-observer variability using these counting rules, the following adapted counting rules were defined in which every CD31-positive object, no matter how small, should be counted, except suspected CD31-positive monocytes, macrophages, and tumor cells. Furthermore, if CD31-positive objects were connected, they were considered a single object, while the absence of staining defined two or more separate objects. microvessel density was calculated for each sample according to  $QA = \frac{1}{4} P_i P_{Ni} / V_i$ ; ref, with  $i$ , a value from 1 to 15 ROIs, expressed as the number of microvessels per area, with  $N_i$  the number of counted vessels in ROI  $i$  and  $V_i$ , ref the number of grid points hitting tissue in ROI  $i$  <sup>(12)</sup>.

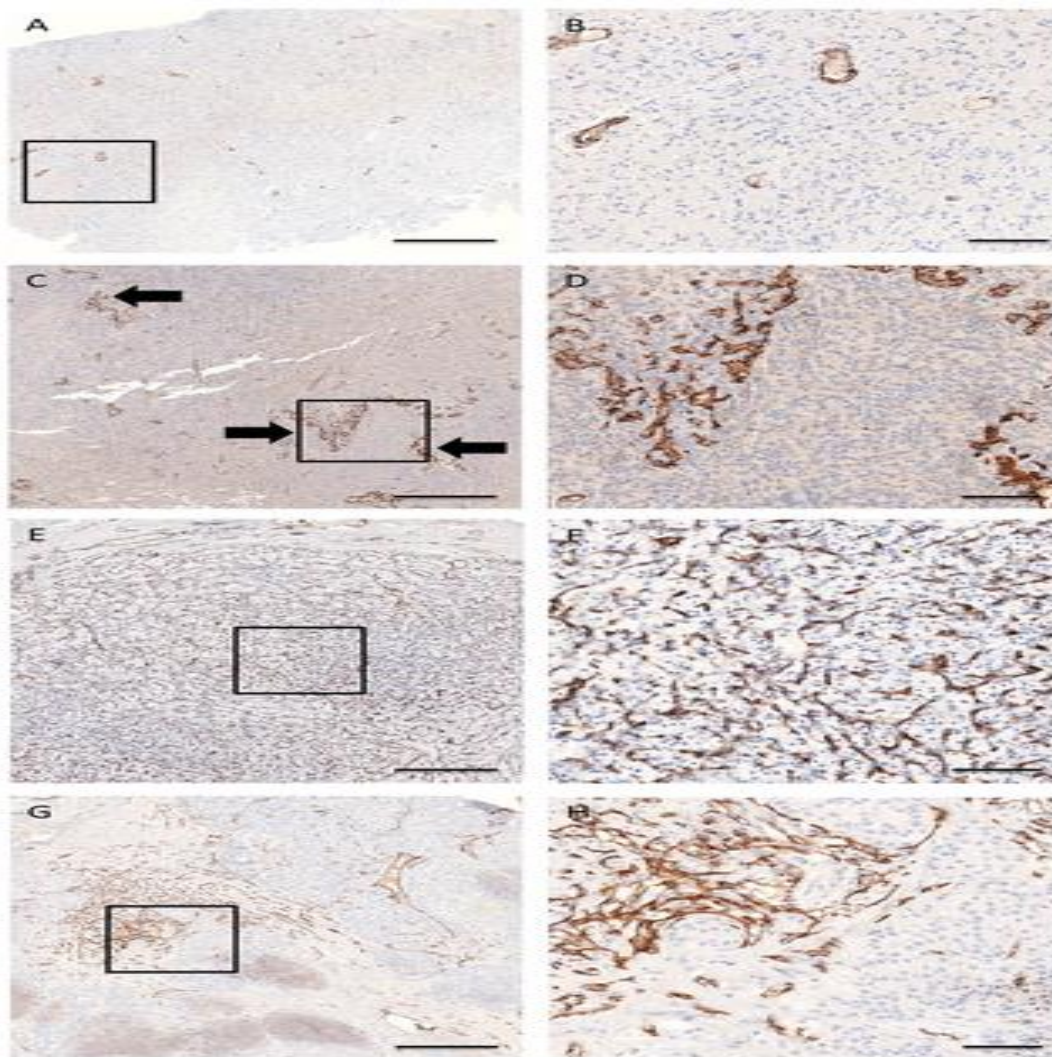


**Figure (2):** Histological heterogeneity of CD31-stained blood vessels in glioblastoma multiforme (a-d) and renal cell carcinoma (e-h). (a-b) QA = 15 vessels per mm<sup>2</sup> , AA = 1.56%, (c-d) QA = 77 vessels per mm<sup>2</sup> , AA = 3.70%, (e-f) QA = 183 vessels per mm<sup>2</sup> , AA = 13.10%, (g-h) QA = 81 vessels per mm<sup>2</sup> , AA = 6.17%. Low (a, b, e, f) heterogeneous samples showed a uniform distribution of vessel profiles as compared to high (c, d, g, h) heterogeneous samples. In glioblastoma multiforme, hotspots and garlands (arrows) were more easily recognized in heterogeneous than in homogeneous samples. Scale bar represents 500  $\mu$ m (a, c, e, g) or 100  $\mu$ m (b, d, f, h).

**Statistical analysis:**

Statistical analysis was performed using SPSS® software for Windows, ver. 20. Variables are reported as means  $\pm$  standard deviations, ranges, and frequencies. The cross-correlations between discrete variables —MRI features and histological features—were analyzed with the chi-squared test. A *p*-value less than or equal to 0.05 was considered statistically significant.

**RESULTS**

**Table (1):** Demographic characteristics of the patients.

| Parameter               | Level             | Percentage | Chi <sup>2</sup> |
|-------------------------|-------------------|------------|------------------|
| Number of patients      | 103               |            |                  |
| Age                     |                   |            |                  |
| Minimum – Maximum Range | 20 – 88<br>(68)   |            |                  |
| Mean $\pm$ SD           | 67.50 $\pm$ 13.56 |            |                  |
| Sex                     |                   |            |                  |
| Male                    | 75                | 72.82      | 8.25**           |
| Female                  | 28                | 27.19      |                  |

\*\* = Significant at (P < 0.01), Our results on the demographic characteristics of the patients cleared that, the number of patients was 103 patients suffer from HCC and the age of these patients ranged from 20 – 88 years with an average of 67.50 years. Most of the patients related to male 75 (72.82 %) and the female reached 28 (27.19 %) (Table 1).

**Table (2):** Type of pre-operative therapy and primary operation applied to patients.

| Parameter                                       | Level | %     | Chi <sup>2</sup> |
|---|-------|-------|------------------|
| <b>Pre-operative therapy</b>                    |       |       |                  |
| No  | 90    | 87.74 | <b>10.25**</b>   |
| Yes   | 13    | 12.26 |                  |
| <b>Type of primary operation</b>                |       |       |                  |
| Atypical resection segment 6.8                  | 15    | 14.56 | <b>25.30**</b>   |
| Central liver resection and hepaticojejunostomy | 3     | 2.91  |                  |
| Extended right hepatectomy                      | 9     | 8.74  |                  |
| Lap atypical                                    | 3     | 2.91  |                  |
| Lap conv  | 2     | 1.94  |                  |
| Lap left lateral sectionectomy                  | 5     | 4.85  |                  |
| Lap segment 6 sectionectomy                     | 2     | 1.94  |                  |
| Laparoscopic left lateral sectionectomy         | 13    | 12.62 |                  |
| Left hepatectomy                                | 5     | 4.85  |                  |
| Left lateral sectionectomy + cholecystectomy    | 8     | 7.77  |                  |
| Liver resection seg 4/5                         | 6     | 5.83  |                  |
| No resection- mets to the falciform ligament    | 2     | 1.94  |                  |
| Resection abandoned due to mets in segment 2    | 3     | 2.91  |                  |
| Right hepatectomy                               | 19    | 18.45 |                  |
| Right posterior sectionectomy                   | 2     | 1.94  |                  |
| Segmental resection seg 4                       | 6     | 5.84  |                  |

\*\* = Significant at (P < 0.01)

Our results on the primary operations cleared that, the number of patients that, take pre-operative therapy reached to 13 (12.26 %). The most primary operation that carried-out to the patients of HCC ranged from right hepatectomy 19 (18.45 %), atypical resection seg 6.8 , 15 (14.56 %) and Laparoscopic left lateral sectionectomy 13 (12.62 %) and the lower operation treatment level lap conv, lap conv 2 (1.94 %), lap segment 6 sectionectom 2 (1.94 %), No resection- mets to falciform ligament 2 (1.94 %) and right posterior sectionectomy 2 (1.94 %) (Table 2).

**Table (3):** Differentiation of HCC among examined patients.

| Parameter                         | Level | %    | Chi <sup>2</sup> |
|-----------------------------------|-------|------|------------------|
| <b>Differentiation</b>            |       |      |                  |
| HCC with mixed hepatobiliary type | 1     | 0.97 | <b>11.42**</b>   |
| Mod                               | 55    | 53.4 |                  |
| N/A                               | 6     | 5.83 |                  |
| Poor                              | 24    | 23.3 |                  |
| Well                              | 17    | 16.5 |                  |

\*\* = Significant at (P < 0.01)

Our results on table (3) on the differentiation of HCC among examined patients cleared that, Mod reached to 55 (53.40 %), poor 24 (23.30 %), well 17 (16.50 %), N/A 6 (5.83 %).

**Table (4):** Lesion number among examined patients.

| Parameter            | Level | %     | Chi <sup>2</sup> |
|----------------------|-------|-------|------------------|
| <b>Lesion number</b> |       |       |                  |
| .00                  | 20    | 19.42 | <b>9.35**</b>    |
| 1.00                 | 68    | 66.02 |                  |
| 2.00                 | 11    | 10.68 |                  |
| 3.00                 | 1     | 0.97  |                  |
| 4.00                 | 1     | 0.97  |                  |
| 5.00                 | 1     | 0.97  |                  |
| 16.00                | 1     | 0.97  |                  |

\*\* = Significant at (P < 0.01)

Our results on the number of lesions cleared that, the number of lesions ranged from 1 in number that observed in 68 (66.02 %) and 2 that observed in 11 (10.68 %), followed by 3, 4, and 5 lesions that observed in 1 (0.97 %) of the examined patients (table 4).

**Table (5):** Location of the lesions among examined patients.

| Parameter                            | Level | %     | Chi <sup>2</sup> |
|--------------------------------------|-------|-------|------------------|
| <b>Location of lesions</b>           |       |       |                  |
| N/A                                  | 2     | 1.94  | <b>25.29**</b>   |
| 5/4 on the middle hepatic vein       | 55    | 53.4  |                  |
| Around portal pedicle at liver hilus | 2     | 1.94  |                  |
| Left lateral liver                   | 4     | 3.88  |                  |
| Right liver                          | 5     | 4.86  |                  |
| Right liver V, VI, VII and VIII      | 1     | 0.97  |                  |
| Right lobe and segment 4             | 2     | 1.94  |                  |
| Rt lobe                              | 16    | 15.54 |                  |
| Segment 2/3                          | 10    | 9.71  |                  |
| Segment 2/3 and segment 5/6          | 1     | 0.97  |                  |
| Segment 5/6                          | 2     | 1.94  |                  |
| Segment 6/7                          | 1     | 0.97  |                  |
| Segment 4/5                          | 1     | 0.97  |                  |
| Segment 3                            | 1     | 0.97  |                  |

\*\* = Significant at (P < 0.01)

Our results on the location of the lesions cleared that, the location of the lesions differ significantly among examined patients (P < 0.05). The higher incidences of the lesions observed in middle hepatic vein 55 (53.40 %) right lobe of the liver 16 (15.54 %) , seg 2/3 10 (9.71 %), right liver 5 (4.86 %), left liver 5 (4.86 %) and in left lateral liver 4 (3.88 %) (Table 5).

**Table (6):** Clearance margin of the lesion among the examined patients.

| Parameter                              | Level | %     | Chi <sup>2</sup> |
|--|-------|-------|------------------|
| <b>Clearance margin</b>                |       |       | 29.30            |
| 1mm                                    | 1     | 0.97  | **               |
| R0                                     | 76    | 73.78 |                  |
| R0 1.5mm                               | 1     | 0.97  |                  |
| R0 but met disease on node samples     | 1     | 0.97  |                  |
| R0 tumor in the vein                   | 1     | 0.97  |                  |
| R1                                     | 14    | 13.60 |                  |
| R1 0.8mm                               | 1     | 0.97  |                  |
| R1 (0.5mm)                             | 1     | 0.97  |                  |
| R1 + peritoneal mets                   | 1     | 0.97  |                  |
| R1 multiple satellite lesion           | 1     | 0.97  |                  |
| R1- tumor ruptured through the capsule | 1     | 0.97  |                  |

\*\* = Significant at (P < 0.01)

Our results on the clearance margin of the lesions differ significantly among patients (P < 0.05). As it showed a higher level in R0 76 (73.78 %) followed by R1 14 (13.60 %) and n/a 3 (2.92 %) (Table 6).

The radiologic findings of the 37 lesions were compared with the pathologic findings to determine the predictability of actual necrosis by imaging. Table (7) presents the degree of histologic necrosis in lesions according to the response observed by WHO criteria. PR, SD, and PD after radioembolization were found to have complete histologic necrosis in 78%, 53%, and 0% of the lesions, respectively.

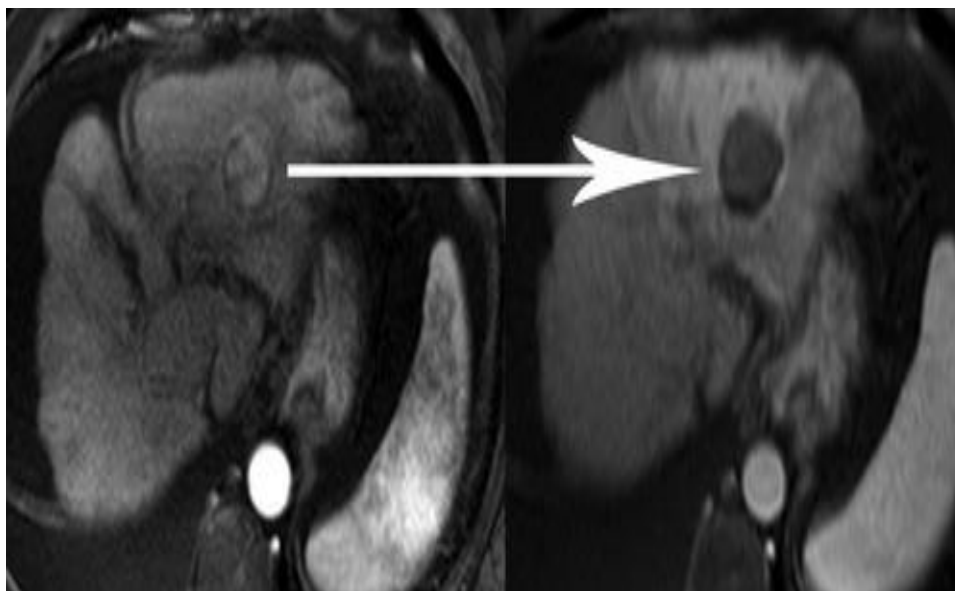
Table (7) presents the degree of histologic necrosis seen in lesions according to the enhancement characteristics observed in the treated lesions. No enhancement, thin rim enhancement, and peripheral nodular enhancement exhibited 100%, 93%, and 38% complete histologic necrosis, respectively.

Table (7) presents the degree of histologic necrosis observed in lesions according to the response by the EASL necrosis criteria. CR, PR, and SD after Y had complete histologic necrosis in 100%, 52%, and 0% of the lesions, respectively. Figures (3) and (4) demonstrate an example of radiologic-pathologic correlation.

**Table (7):** Histologic Necrosis According to WHO/Enhancement Characteristics/ EASL.

| WHO Response                | n (%)             |                      |                                | P-Value |
|-----------------------------|-------------------|----------------------|--------------------------------|---------|
|                             | Partial Response  | Stable Disease       | Progressive Disease            |         |
| Total number                | 20/37 (54)        | 18/37 (48)           | 3/37 (8)                       |         |
| Histologic necrosis, n (%)  |                   |                      |                                |         |
| 100%                        | 15 (78)           | 9 (53)               | 0 (0)                          | 0.77    |
| >50%                        | 4 (17)            | 5 (29)               | 2 (50)                         |         |
| <50%                        | 1 (5)             | 4 (18)               | 1 (50)                         |         |
| Enhancement Characteristics | n (%)             |                      |                                | P-Value |
|                             | No Enhancement    | Thin Rim Enhancement | Peripheral Nodular Enhancement |         |
| Total number                | 3/37 (14)         | 16/37 (38)           | 22/37 (57)                     |         |
| Histologic necrosis, n (%)  |                   |                      |                                |         |
| 100%                        | 3 (100)           | 13 (93)              | 8 (38)                         | 0.104   |
| >50%                        | 0 (0)             | 3 (7)                | 8 (38)                         |         |
| <50%                        | 0 (0)             | 0 (0)                | 6 (24)                         |         |
| EASL Response               | n (%)             |                      |                                | P-Value |
|                             | Complete Response | Partial Response     | Stable Disease                 |         |
| Total number                | 12/37 (32)        | 25/37 (57)           | 4/37 (11)                      |         |
| Histologic necrosis, n (%)  |                   |                      |                                |         |
| 100%                        | 12 (100)          | 11 (52)              | 0 (0)                          | 0.0042  |
| >50%                        | 0 (0)             | 11 (38)              | 1 (25)                         |         |
| <50%                        | 0 (0)             | 3 (10)               | 3 (75)                         |         |

Abbreviations: EASL, European Association for the Study of the Liver; WHO, World Health Organization.



**Figure (3):** Pre- and post-treatment magnetic resonance imaging showing EASL complete response (arrow).

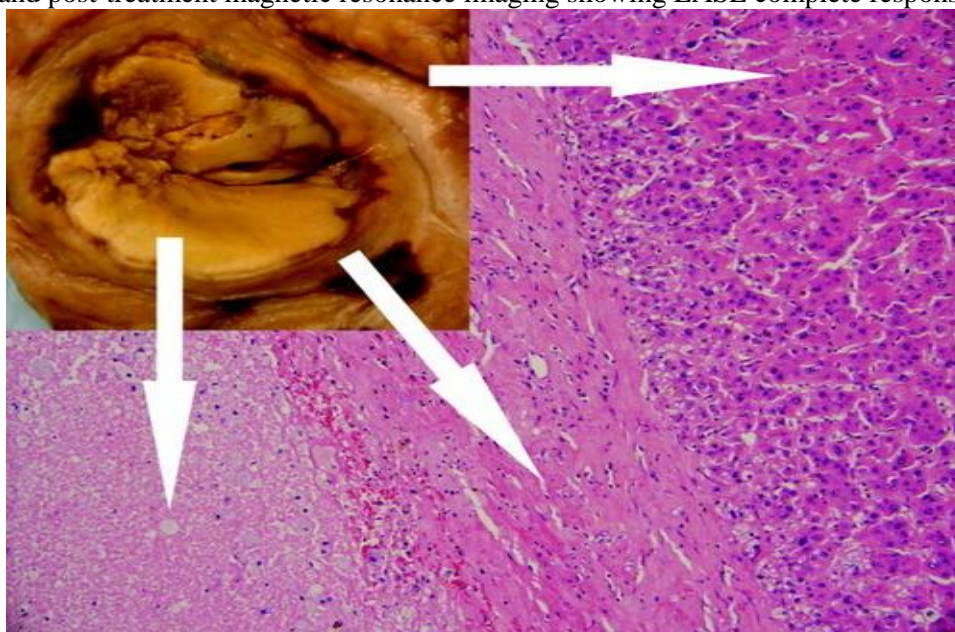


**Figure (4):** Gross and histologic correlation. In a clockwise direction, arrows demonstrate normal parenchyma, fibrosis (peripheral rim), and completely necrotic tumor.

## DISCUSSION

Our results on the demographic characters of the patients cleared that, the number of patients was 103 patients suffer from HCC and the age of these patients ranged from 20 – 88 years with an average of 67.50 years. Most of the patients related to male 75 (72.82 %) and the female reached 28 (27.19 %). These results attributed to them by increasing the age there is a decrease of immunity of patients against different diseases and risk factors that causes the HCC, and by the nature of the work activities by the male that expose them to many risk factors that cause a higher incidence to the HCC.

These results agreed with those of **Tokushige *et al.*** <sup>(14)</sup>, where they concluded that hepatocellular carcinoma most commonly occurs in the middle and old age group with a predominance of male.

While, our results on the primary operations cleared that, the number of patients that, take pre-operative therapy reached to 13 (12.26 %). The most primary operation that carried-out to the patients of HCC ranged from Right hepatectomy 19 (18.45 %), Atypical resection seg 6.8 , 15 (14.56 %) and Laparoscopic left lateral sectionectomy 13 (12.62 %) and the lower operation treatment level Lap conv , Lap conv 2 (1.94 %), Lap segment 6 sectionectom2 (1.94 %), No resection- mets to falciform ligament 2 (1.94 %) and Right posterior sectionectomy 2 (1.94 %).

Our results agreed with those of **Belghiti and Kianmanesh** <sup>(15)</sup> where they reported that the Surgery for hepatocellular carcinoma (HCC) includes partial liver resection (LR) and liver transplantation (LT). Although LT represents the most efficient treatment in patients with small HCC, <30% of patients are eligible

for LT because of restrictive criteria (one nodule <5 cm or two to three nodules <3 cm without macroscopic vascular invasion), graft unavailability and the high cost of the procedure. For large HCC, LR remains the only potentially curative treatment. LR is now safer, with a low rate of mortality.

Also, our results on the differentiation of HCC among examined patients cleared that, the differentiation of HCC among examined patients cleared that, Mod reached to 50 (48.55 %), poor 23 (22.34 %), well 15 (14.56 %), and Mod to poor 3 (2.91 %).

While, our results on the size of the lesions cleared that, the size of lesion ranged from (10 mm - 2.5 Cm) with an average of (45 X 45 X 30 mm). also, our results on the Lesion number among examined patients cleared that, the number of lesions ranged from 1 in number that observed in 68 (66.02 %) and 2 that observed in 11 (10.68 %), followed by 3, 4, and 5 lesions that observed in 1 (0.97 %) of the examined patients.

These results agreed with those of **Pomfret *et al.***<sup>(16)</sup>, where they reported that the size and number of tumors, which together represent tumor burden, are important prognostic factors for HCC. The availability and success of curative treatment options, such as liver resection or transplantation, depends heavily on the size and number of HCCs. Patients with one 2-5-cm HCC nodule or 2 to 3 HCC nodules measuring < 3 cm, who have no macrovascular invasion or extrahepatic metastases, have priority for transplantation

Our results on the location of the lesions cleared that, the location of the lesions differ significantly among examined patients ( $P < 0.05$ ). The higher incidences of the lesions observed in middle hepatic vein 55 (53.40 %) right lobe of the liver 16 (15.54 %), seg 2/3 10 (9.71 %), right liver 5 (4.86 %), left liver 5 (4.86 %) and in left lateral liver 4 (3.88 %). Our results agreed with those of **Song *et al.***<sup>(17)</sup> where they observed that by using magnetic resonance sound (MRI) we can detect the different sits of the lesions in the liver due to HCC where they observed that, all patients (52/52, 100%) showed HV lesions of different degrees. MRV was inferior to the US in detecting cord-like occlusions (6 vs. 19,  $\chi^2 = 11.077$ ,  $p < 0.001$ ). Dilated AHVs, including 50 (50/52, 96.2%) caudate lobe veins and 37 (37/52, 71.2%) inferior HV and AHV lesions, were well-detected. There were no significant differences in detecting segmental lesions and thrombosis between MRV and DSA ( $\chi^2 = 0.000$ ,  $p_1 = 1.000$ ,  $p_2 = 1.000$ ). The capacity of MRV to detect membranous lesions was inferior to that of DSA (7 vs. 15,  $\chi^2 = 6.125$ ,  $p = 0.013$ ).

Also, the pathogenesis of venous lesions indicates that obstructions can be located in all HVs, and this involvement usually occurs asynchronously and progresses at variable speeds<sup>(18)</sup>. Imaging can reveal obstructions in HVs and the IVC, including the site and extent of the obstructions, as well as the draining conditions of emerging collateral pathways; therefore,

imaging is an important procedure for diagnosing BCS. The value of ultrasound and angiography in diagnosing BCS has been well studied and confirmed<sup>(17)</sup>.

While, our results on the Haematological changes among examined patients cleared that, there is a significant decrease in the level of RBCs, WBCs, platelets level, APTT, PTT. While, our results on the biochemical changes among examined patients cleared that, there is a significant increase in the level of Bilirubin, ALT, ALP, Albumin, Urea, and creatinine than the normal level.

This results also confirmed by our results on the correlation between the pathological and radiological methods, that indicated that there is a negative correlation between Hb level, RBCs, platelets level, PTT, Albumin, Creatinine with incidences of HCC indicators that diagnosed by radiological methods. Also, our results cleared that, there are positive correlations between WBCs, Activated partial thromboplastin time (APTT), bilirubin (mg/dL), ALP, GGT, urea, INR, and AFP. Also, our results cleared that, there are positive correlations between WBCs. These results indicated that the hematological and biochemical examinations confirm the results of MRI and CT for diagnosing the HCC and the determination of its prognosis and treatment. While, our results on the INR and AFP cleared that, the level of INR ranged from 0.00 to 1.50 with a mean value of 0.99. While, our results on the AFP cleared that, the level of AFP ranged from 0.00 to 85328.00 with a mean value of 1204.05.

These results agreed with those of **Vasuri *et al.***<sup>(19)</sup>, where they concluded that many advances have been made in the imaging diagnosis and the histopathological evaluation of HCC. However, the classic imaging and histopathological features of HCC are still inadequate to define the patient's prognosis. We aimed to find the link between new proposed morphovascular patterns of hepatocellular carcinoma (HCC) and magnetic resonance imaging (MRI) features to identify pre-operative markers of biologically aggressive HCC. Thirty-nine liver nodules in 22 patients were consecutively identified. Histopathological analysis and immunohistochemistry for CD34 and Nestin were performed to identify the four different HCC morphovascular patterns. MRI was performed using gadolinium ethoxybenzyl diethylenetriamine pentaacetic acid. Three out of four morphovascular HCC patterns showed peculiar MRI features: in particular Pattern D (solid aggressive HCCs with CD34+/Nestin+ new-formed arteries) were isointense on T1-WI in 83% of cases and hyperintense on T2-WI in 50%. Five histologically-diagnosed HCC were diagnosed as non-malignant nodules on MRI due to their early vascularization and low aggressiveness (Pattern A). The comparison between histology and MRI confirms that a subclassification of HCC is possible in a pre-operative setting. MRI seems to reinforce once more the identity

of the different morphovascular HCC patterns and the possibility to pre-operatively identify HCCs with features of biological aggressiveness.

## CONCLUSION

**This study concluded that,** the association between the Imaging and pathological features of HCC including microvascular invasion and density which is very important for getting an honest designation on the lesions of HCC and for getting the best treatment and prognosis of this lesions.

## RECOMMENDATIONS

So we **recommend** to carry-out two methods of diagnosis that include, diagnostic tomography, and pathological diagnosis with microvascular counting for obtaining the best idea about the diagnosis, prognosis, and treatment of the HCC.

## REFERENCES

1. **Forner A, Reig M, Bruix J (2018):** Hepatocellular carcinoma. *Lancet*, 391:1301–1314.
2. **Kim JH, Joo I, Lee JM (2019):** Atypical Appearance of Hepatocellular Carcinoma and Its Mimickers: How to Solve Challenging Cases Using Gadoteric Acid-Enhanced Liver Magnetic Resonance Imaging. *Korean J Radiol.*, 20(7):1019-1041.
3. **Tang A, Cruite I, Mitchell D, Sirlin C (2018):** Hepatocellular carcinoma imaging systems: why they exist, how they have evolved, and how they differ. *Abdom Radiol (NY)*, 43:3–12.
4. **Elsayes KM, Hooker JC, Agrons MM, Kielar AZ, Tang A, Fowler KJ et al. (2017):** 2017 version of LI-RADS for CT and MR imaging: an update. *Radiographics*, 37:1994–2017.
5. **Cha DI, Jang KM, Kim SH, Kang TW, Song KD (2017):** Liver Imaging Reporting and Data System on CT and gadoteric acid-enhanced MRI with diffusion-weighted imaging. *Eur Radiol.*, 27:4394–4405.
6. **Choi JY, Lee JM, Sirlin CB (2014):** CT and MR imaging diagnosis and staging of hepatocellular carcinoma: part II. Extracellular agents, hepatobiliary agents, and ancillary imaging features. *Radiology*, 273:30–50.
7. **Fraum TJ, Tsai R, Rohe E, Ludwig DR, Salter A, Nalbantoglu I et al. (2018):** Differentiation of hepatocellular carcinoma from other hepatic malignancies in patients at risk: diagnostic performance of the Liver Imaging Reporting and Data System version 2014. *Radiology*, 286:158–172.
8. **Yoneda N, Matsui O, Kitao A, Kozaka K, Kobayashi S, Sasaki M et al. (2016):** Benign hepatocellular nodules: hepatobiliary phase of gadoteric acid-enhanced MR imaging based on molecular background. *Radiographics*, 36:2010–2027.
9. **European Association for the Study of the Liver (2018):** EASL Clinical Practice Guidelines: Management of hepatocellular carcinoma. *J Hepatol.*, 69:182–236.
10. **Chernyak V, Santillan C, Papadatos D, Sirlin C (2018):** LI-RADS® algorithm: CT and MRI. *Abdom Radiol (NY)*, 43:111–126.
11. **Tang A, Bashir M, Corwin M, Cruite I, Dietrich C, Do R et al. (2018):** LI-RADS Evidence Working Group. Evidence supporting LI-RADS major features for CT- and MR imaging-based diagnosis of hepatocellular carcinoma: a systematic review. *Radiology*, 286:29–48.
12. **Marien KM, Croons V, Waumans Y, Sluydts E, De Schepper S, Andries L et al. (2016):** Development and Validation of a Histological Method to Measure Microvessel Density in Whole-Slide Images of Cancer Tissue. *PLoS ONE*, 11(9): e0161496.
13. **Gundersen HJ, Bendtsen TF, Korbo L, Marcussen N, Møller A, Nielsen K et al. (1988):** Some new, simple and efficient stereological methods and their use in pathological research and diagnosis. *APMIS.*, 96: 379–94.
14. **Tokushige K, Hashimoto E, Yatsuji S et al. (2010):** Prospective study of hepatocellular carcinoma in nonalcoholic steatohepatitis in comparison with hepatocellular carcinoma caused by chronic hepatitis C. *J Gastroenterol.*, 45(9):960–967.
15. **Belghiti J, Kianmanesh R (2005):** Surgical treatment of hepatocellular carcinoma. *HPB (Oxford)*, 7(1):42-9.
16. **Pomfret EA, Washburn K, Wald C, Nalesnik MA, Douglas D, Russo M et al. (2010):** Report of a national conference on liver allocation in patients with hepatocellular carcinoma in the United States. *Liver Transpl.*, 16:262–278.
17. **Song RX, Cai SF, Ma S, Liu ZL, Gai YH, Zhang CQ, Wang GC (2018):** Magnetic Resonance Venography Findings of Obstructed Hepatic Veins and the Inferior Vena Cava in Patients with Budd-Chiari Syndrome. *Korean J Radiol.*, 19(3):381-388.
18. **Valla DC (2009):** Primary Budd-Chiari syndrome. *J Hepatol.*, 50:195–203.
19. **Vasuri F, Renzulli M, Fittipaldi S, Brocchi S (2019):** Pathobiological and Radiological Approach For Hepatocellular Carcinoma Subclassification. *Scientific Reports*, 9:14749. <https://doi.org/10.1038/s41598-019-51303-9>.